JOURNAL OF AIRCRAFT
Vol. 31, No. 1, Jan.–Feb. 1994

Aerodynamics of Airfoils with Vortex Trapped by Two Spanwise Fences

Vernon J. Rossow*
NASA Ames Research Center, Moffett Field, California 94035

The research described here is part of a general effort to find simple ways by which wings of aircraft can be converted from an efficient cruise configuration to one that develops the high lift needed during landing and takeoff. The particular high-lift concept studied here consists of a conventional airfoil with a vortex trapped over the upper surface. The vortex is trapped by one or two vertical fences that serve as barriers to the oncoming stream and as reflection planes for the vortex and the sink that form an organized separation bubble on top of the airfoil. In order to illustrate the concept for two-dimensional configurations, computed results are presented for the flow over a Clark-Y airfoil for a variety of fence geometries and angles of attack to determine the aerodynamic characteristics of these trapped-vortex, high-lift devices. Even though the results presented here are for two-dimensional inviscid and incompressible flow, the results provide a beginning data base for the characteristics of trapped-vortex airfoils for possible application as high-lift devices on swept-wing aircraft.

Nomenclature

C_d = section drag coefficient, D/qc
C_ℓ = section lift coefficient, L/qc
C_m = pitching-moment coefficient, M/qc^2
c = wing chord or characteristic length
D = drag due to flow into sink/unit span
h = step or fence height
L = lift/unit span
M = pitching moment about quarter-chord/unit span
$\dot{m}$ = strength of external source
q = dynamic pressure, $\rho U_\infty^2/2$
r = radius
r_{oc} = radius of circle in original or circle plane
U_∞ = freestream velocity
u, v = dimensionless velocity components
x, y = distance in streamwise and vertical directions
z = complex variable, $x + iy$
$\bar{z}$ = $x - iy$
α = angle of attack
α_0 = -0.05906 rad, angle of zero lift
β_c = airfoil curvature parameter
β_{rk} = fence curvature parameter
Γ = circulation in external vortex
Γ_o = circulation at center of circle in z_o plane
δ = thickness parameter in Joukowski mapping
θ = meridian angle
τ = included angle of trailing edge
Φ = complex potential, $\phi + i\psi$
ϕ = velocity potential
ψ = stream function

Subscripts

f = front fence
ix = location of image vortex in original plane
o = original plane
ox = location of trapped vortex in original plane
p = physical plane
px = location of trapped vortex in physical plane
r = rear fence

Received Sept. 3, 1991; presented as Paper 91-3269 at the AIAA 9th Applied Aerodynamics Conference, Baltimore, MD, Sept. 23–25, 1991; revision received Oct. 22, 1992; accepted for publication Nov. 30, 1992.

*Senior Scientist. Associate Fellow AIAA.

Introduction

AIRCRAFT with highly swept wings usually land and takeoff at high angles of attack in order to achieve the lift needed to support their weight at low speeds. At the required angles of attack, a long fuselage necessitates long landing gear. Much of the problem is removed if the needed lift is developed at angles of attack near those flown during cruise. In order to achieve this goal, a research program has been underway at NASA Ames Research Center to develop mechanisms that will provide the needed high lift on a wing at low to moderate angles of attack. The high-lift concept that is the subject of this article uses conventional airfoils with a vortex trapped above the upper surface of the wing. The vortex is trapped by one or two spanwise fences that serve as barriers to the oncoming stream and as reflection planes for both the vortex and the sink. The purpose of the trapped vortex is to introduce additional thickness and camber into the effective aerodynamic shape of the wing. The study is therefore directed at finding design guidelines for the construction of wings so that they will trap a strong spanwise vortex above their upper surface.

A review of the literature[1–23] indicates that a wide variety of configurations have been proposed which employ either a rotating cylinder,[1–7] or a vortex, in order to increase substantially the circulation or lift on the wing. Some of the configurations proposed were able to develop section lift coefficients over 8. The mechanical difficulties with driving a rotating cylinder, and the inefficiency of the system when not in use, drove the conceptual process toward the use of vortices trapped inside free-streamline regions over the upper surface of the wing.[8–13] Different combinations of surfaces were tried to enhance and stabilize the vortex. One such concept proposed by Kasper[10–15] was tried on an aircraft with some success.[13] Various computations[16–19] showed that vortices could be established on the upper surface of a wing to produce lift coefficients up to 10. Wind-tunnel experiments[20–23] indicated, however, that the measured lift coefficients did not approach those predicted by the various theories, or those obtained with rotating cylinders.

The material presented in this article is an extension of the trapped-vortex studies[24,25] that begin the development of

guidelines for the establishment of vortices trapped over airfoils for the high lift needed for landing and takeoff. This article presents the characteristics of airfoils with trapped vortices in order to determine the variation of fence height with airfoil angle of attack, location of fences, and other parameters. The two-dimensional flowfield is assumed to be inviscid, incompressible, and in the final steady state so that it can be represented by potential flow theory using the superposition of singularities.

Guidelines for Trapping Vortices on Airfoils

The full three-dimensional flow over the wing of an aircraft is so complicated that it is hard to get an understanding of the principles that govern the vortex-trapping process. Therefore, the analysis is first restricted to a two-dimensional section of the flowfield which is approximated by the device illustrated in Fig. 1. As shown, the customary flow about an airfoil is assumed to also contain a spanwise vortex located between the suction orifices in the end plates. A spanwise fence or spoiler located near the nose of the airfoil initially sheds a shear or vortical layer that is concentrated into the spanwise vortex by withdrawal of fluid at the suction orifices. As the vortex strength increases with time, the organized rotational flow, or vortex, eventually builds to the point where the vortex dominates the entire separated flow region, changing it from a region of random motions to one occupied by a well-organized vortex. The flow then leaves the tip of the front fence without shedding a shear layer. At that point, the vortex reaches its maximum strength. If the location of the vortex center is at its equilibrium point, all of the induced velocity contributions at its center sum to zero so that the vortex is stationary and the flowfield steady.

The simplified experimental configuration shown in Fig. 1 is approximated by the two-dimensional theoretical model illustrated in Fig. 2a. A large trapped-vortex bubble is shown over the airfoil to emphasize the fact that the study is most interested in those configurations wherein the vortex bubble covers a large fraction of the upper surface of the airfoil. If such a flowfield can be established, enhancement of the lift of the airfoil by the trapped vortex is enough to yield lift coefficients[16,18,19,24] up to $C_\ell = 10$. As indicated in Fig. 2, the flow is assumed to depart smoothly from both the tip of the front fence and from the trailing edge of the airfoil in order to satisfy the Kutta condition at those locations. Conformal mapping techniques are then used to develop the desired flowfield configuration from the flow about a circular cylinder (Fig. 2b). A substantial advantage of the conformal mapping technique is that it yields directly the location of the equilibrium point for the center of the vortex/source combination, the circulation Γ of the vortex, and the source strength $\dot{m}$. Knowledge of Γ and $\dot{m}$ then yield the lift on the airfoil and the drag attributed directly to the trapping process by the equations

$$C_\ell = -2.0(\Gamma + \Gamma_o)/cU_\infty \tag{1}$$

$$C_d = -2.0\dot{m}/cU_\infty \tag{2}$$

The foregoing discussion explains why a front fence is needed in the generation of the trapped vortex. The need for a second fence downstream of the trapped vortex was not apparent until sometime after the completion of an analysis that employed only a front fence.[24] In this earlier theoretical study of the characteristics of trapped-vortex airfoils, it was predicted that a sizable sink flow at the vortex center is required in order to achieve the zero-velocity or equilibrium condition for the vortex. Experiments[24] with models that resemble the configuration presented in Fig. 1 confirmed that the equilibrium condition did indeed require a large mass flow removal at the vortex axis when only a front fence is used. In practice, mass flow removal is accomplished by flow spanwise along

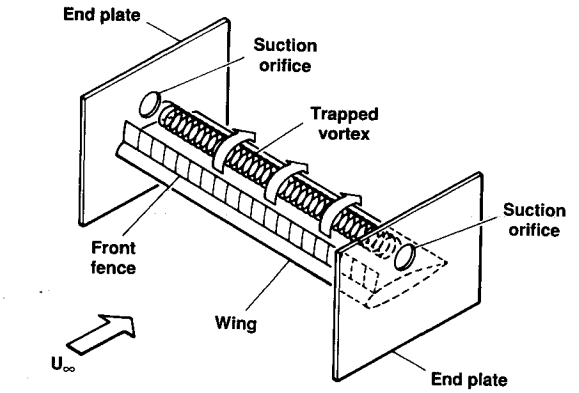

Fig. 1 Diagram of experiment that represents two-dimensional trapped-vortex concept on a wing.

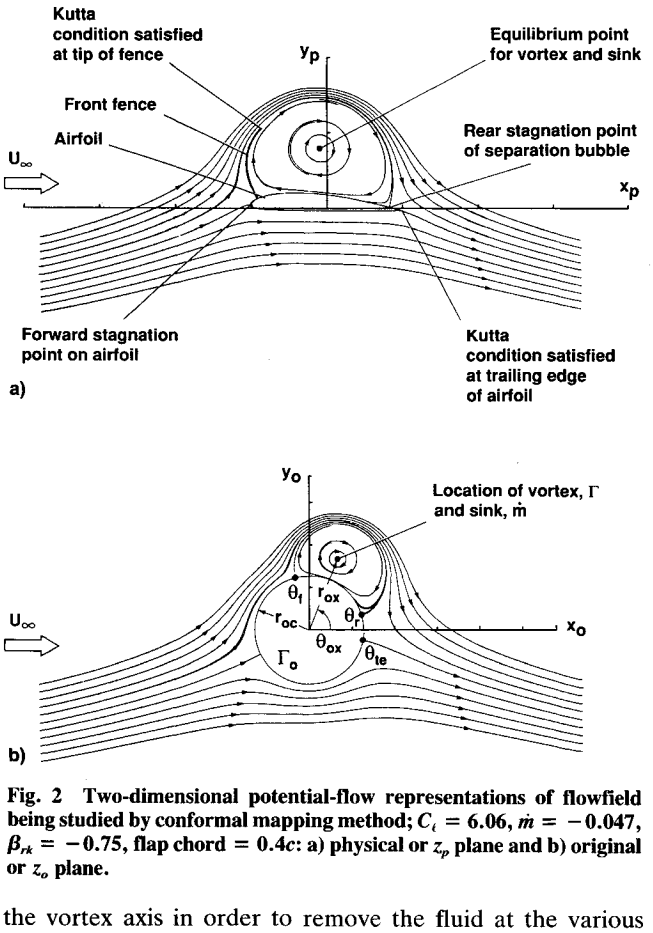

Fig. 2 Two-dimensional potential-flow representations of flowfield being studied by conformal mapping method; $C_\ell = 6.06$, $\dot{m} = -0.047$, $\beta_{rk} = -0.75$, flap chord $= 0.4c$: a) physical or z_p plane and b) original or z_o plane.

the vortex axis in order to remove the fluid at the various spanwise stations. Flow visualization using dye filaments indicated that the axial flow was sometimes so large that the entire trapped-vortex region consisted of spanwise rather than vortex flow. Furthermore, since the fluid traveling along the vortex axis gives up its streamwise momentum, a drag is associated with the sink flow. This drag is called the vortex-trapping drag because it is directly attributable to the vortex-trapping process.

The results described in the foregoing paragraph indicate that the flowfield pictured in Figs. 1 and 2 needs to be modified in some way if the equilibrium condition, and therefore, vortex trapping, is to be achieved with negligible drag (or zero sink flow) at the vortex axis. Since it was not obvious how to find the configuration changes that would produce vortex trapping with zero sink flow, a two-dimensional, inviscid, incompressible flow analysis[25] was carried out on a variety of simple flowfield configurations. As solutions for the various configurations were found, a method became apparent whereby the source flow could be made to vanish and still have an

equilibrium point for the vortex. Quite simply, it was found that a combination of upstream and downstream fences can be used to reduce to zero the sink flow required for equilibrium. The interactions of the trapped vortex with both vertical and horizontal surfaces are illustrated in Fig. 3. In order to explain the need for a second fence, consider the two-fence trapped-vortex configuration as three separate flat-plate boundaries. The horizontal flat plate serves as a reflection plane with an image vortex below the surface which induces an upstream velocity on the vortex that is exactly equal to the oncoming freestream velocity. If the fences were not present, this configuration by itself would yield an equilibrium point without a source. From practical considerations, a fence of some sort is required upstream of the vortex in order to provide the shear layer and vorticity mentioned previously that builds the circulation in the vortex. Once again, by potential flow theory, the presence of such a vertical boundary induces an upward velocity through the influence of the image vortex needed to make the surface a streamline. The upward velocity due to the front fence needs to be offset by a sink located at the vortex center and an image sink located beneath the horizontal plane, unless some change is made in the flowfield geometry to bring about an equilibrium condition. Such a change is available from a fence downstream of the vortex. As indicated in Fig. 3, the image vortex for the rear fence induces a downward velocity on the vortex. Therefore, if the vortex to be trapped is midway between two vertical surfaces of about the same size, an equilibrium condition is achieved for the vortex without the presence of a source or sink. If the flowfield does not have fore and aft symmetry, the heights of the upstream and downstream fences can be adjusted so that trapped-vortex flowfields can be established over arbitrary shapes with a sink of negligible or zero strength. This design guideline makes it possible to obtain an efficient trapped vortex flowfield.

In summary, the two fences do several things in the flowfield. The front fence serves as an upstream limit on the trapped-vortex flowfield, as a reflection plane for the vortex, and as a means for generating a shear layer that supplies vorticity for the establishment of the trapped vortex. The second fence serves as a downstream limit on the size of the vortex bubble and as a reflection plane for the vortex so that trapping can be achieved without the need for a source or sink. Since a source or sink is no longer required for maintaining an equilibrium point, the drag due to vortex trapping is negligible. This means that efficient lift enhancement has been achieved. Another advantage obtained when trapping has been achieved with negligible sink flow is that the flow along the core of the vortex is also negligible, making it much easier to establish and maintain the vortex flowfield in practice.[26,27] Mass removal from the core is then only necessary to establish the vortex and to remove low energy fluid generated by viscous losses.

The theoretical study reported here was undertaken to determine the characteristics of airfoils with efficient (zero sink strength) trapped vortices. The two-dimensional, inviscid, incompressible flow analysis method is the same one used previously.[24,25] The airfoil chosen is again the Clark-Y (which is nearly the same as the NACA 4412) section. In the presentations to follow, all of the solutions were obtained for the zero-sink situation because they are the ones of interest for application on three-dimensional wings. Hence, after the analysis method has been briefly described, the results from a number of solutions are used to study the characteristics of airfoils that have a vortex trapped between two spanwise fences. The fence heights are designed so that a sink of negligible strength suffices at the equilibrium point. The parameters considered include the size of the vortex bubble, its streamwise location on the airfoil, the minimum fence sizes needed for vortex trapping with zero-sink flow, and the effect of fence curvature on the fence size, lift and pitching moment.

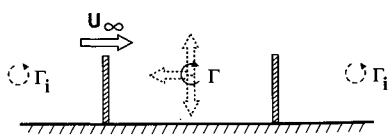

Fig. 3 Image system showing advantage of two-fence concept.

Overview of Analysis Method

Equations and Boundary Conditions

The analysis begins in the original plane where the boundary conditions on a circle are specified (Fig. 2). The circle is a streamline and the location of the three stagnation points at θ_f, θ_r, and θ_{te} on the circle locate the front and the rear limits of the vortex/source bubble, and the trailing edge of the airfoil. The curved fence near the leading edge of the airfoil is produced by use of the same sequence of mapping functions used previously.[24,25] The fence at the rear of the vortex/source bubble is formed by the Joukowski transformation[28] with no special effort made to curve the fence one way or the other. If the rear fence is located near midchord, it is close to a flat plate. If the second fence is aft of the center of the airfoil, the fence will curve aft. Similarly, when the fence is located forward of the center of the airfoil, it tends to have a forward bend.

The complex potential for the flowfield is constructed from a superposition of vortex and source singularities to produce a separation bubble on the outside of a circular boundary (Fig. 2). A vortex (Γ_o) is placed at the center of the circle in the original or z_o plane to represent the circulation on the circle. The complex potential is then given by[24]

$$\Phi = (z_o + r_{oc}^2/z_o) + \frac{\dot{m}}{2\pi U_\infty} \ln[(z_o - z_{ox})(z_o - z_{ix})/z_o] - \frac{i\Gamma}{2\pi U_\infty} \ln \frac{z_o(z_o - z_{ox})}{z_o - z_{ix}} - \frac{i\Gamma_o}{2\pi U_\infty} \ln z_o \tag{3}$$

where r_{oc} is the radius of the circle in the z_o-plane and $z_{ix} = z_{ox}r_{oc}^2/r_{ox}^2$ is the location of the image of the vortex/source combination inside the circle. A vortex and a source are also placed at the center of the circle to compensate for the image singularities. The velocity in the flowfield is then found from

$$u_o - iv_o = (1 - r_{oc}^2/z_o^2) + \frac{\dot{m}}{2\pi U_\infty} \times \left(\frac{1}{z_o - z_{ox}} + \frac{1}{z_o - z_{ix}} - \frac{1}{z_o}\right) - \frac{i\Gamma}{2\pi U_\infty} \times \left(\frac{1}{z_o - z_{ox}} - \frac{1}{z_o - z_{ix}} + \frac{1}{z_o}\right) - \frac{i\Gamma_o}{2\pi U_\infty}\left(\frac{1}{z_o}\right) \tag{4}$$

α of the airfoil relative to the freestream is imposed on the airfoil by several steps in the mapping sequence, as are the fence sizes and their locations. The lift on the basic airfoil vanishes at $\alpha = \alpha_o = -0.05906$ rad. The magnitude and locations of the singularities and the parameters in the mapping process are determined so that 1) the front of the vortex/source bubble maps into the tip of the front fence; 2) the downstream end of the separation bubble maps into the tip of the rear fence; and 3) the point marked θ_{te} in Fig. 2 maps into the trailing edge of the airfoil. The locations of these three points on the circle in the z_o plane are found by mapping backwards from the physical plane through the formation of the two fences to the circle in the original plane. In this way, when the zero velocity condition at the equilibrium point is imposed, there are just enough boundary conditions to tie down the magnitude and location of the vortex/source com-

bination at the equilibrium point and the circulation Γ_o. The relationship between the singularities in the flowfield and the stagnation points is obtained from the circumferential velocity on the surface of the circle in the z_o plane as

$$v_\theta = -2\sin\theta_o + \frac{\dot{m}}{2\pi U_\infty} \times \left[\frac{2r_{ox}\sin(\theta_o - \theta_{ox})}{r_{oc}^2 + r_{ox}^2 - 2r_{oc}r_{ox}\cos(\theta_o - \theta_{ox})}\right] + \frac{\Gamma}{2\pi U_\infty} \times \left\{\frac{2[r_{oc} - r_{ox}\cos(\theta_o - \theta_{ox})]}{r_{oc}^2 + r_{ox}^2 - 2r_{oc}r_{ox}\cos(\theta_o - \theta_{ox})}\right\} + \frac{\Gamma_o}{2\pi U_\infty}\left(\frac{1}{r_{oc}}\right) \quad (5)$$

Method Used to Find Equilibrium Point

The foregoing equations and boundary conditions completely specify the solution, but the strengths of the singularities and the location of the equilibrium point cannot be found explicitly. Therefore, an iterative process is used to find the location and the strengths of the vortex and sink. By a trial and error process, the method that has been developed first scans the flowfield between the fences at discrete points on a mesh in the original or z_o plane. When a point is found wherein the velocity components pass through zero, the search area is reduced to a single unit of the original mesh. The search technique is then repeated on a mesh of smaller size. More precise definition of the location of the equilibrium point is achieved by linear interpolation on the refined mesh. By this method the zero velocity or equilibrium point is found for the vortex center. Figure 4a illustrates the streamlines for the flowfield in the physical plane. A vector representation of the velocity at various points in the physical flowfield is shown in Fig. 4b. The case used in the illustration, Fig. 4a, has a flat fence upstream of the vortex (rather than a conforming fence) and a flat fence downstream of the vortex in order to have two fixed fences, and therefore, symmetry in the flowfield geometry. Typically, the velocity varies in an orderly fashion at radii larger than the radius of the equilibrium point, but as the surface of the airfoil is approached the fluctuations in the magnitude of the velocity increase (Fig. 4b). These variations occur because, in that region, the self-induced velocities increase rapidly and other equilibrium points occur in the corners where the fences intersect the airfoil. These equilibrium points and the ones near the tips of the fences are not of interest here because they require large source strengths. The only equilibrium point that is of interest is the one approximately midway between and near the top of the two fences. It is the one that can most easily be made to occur with a vanishing source strength, and therefore, the one with the greatest practical significance.

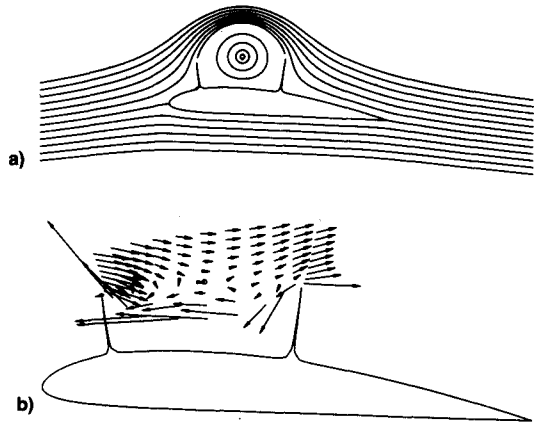

Fig. 4 Flowfield and velocity induced on center of vortex/source combination when at various locations; $C_t = 1.94$, $\beta_{rk} = -0.75$, $x_f/c = 0.134$, $x_r/c = 0.501$, $h_f/c = 0.115$, $h_r/c = 0.150$: a) flowfield and b) vector representation of induced velocity at vortex center.

The display of vectors in Fig. 4b indicates the velocity direction and magnitude induced on the vortex/source combination. The equilibrium point is not necessarily a stable location because a small displacement can lead to a velocity that does not restore the vortex back to its ideal location. In practice,[26,27] it was found that the vortex is much more stable and returns more quickly to its equilibrium position if two fences are present rather than one.

At first there appears to be no physical reason why an equilibrium point cannot be found for any arrangement of airfoil and fence sizes, locations, etc. However, it soon became apparent, both from the previous work[24,25] and in the present study, that definite limits exist for equilibrium solutions. In the present study of two-fence cases, it was found that there is at least one advantage to making the flat part of the fences as large as possible within the range of solutions. It seems that, as both fences increase in size, the equilibrium conditions require that the fences become more nearly the same size. The flowfield then appears to become less sensitive to fence height and curvature. However, it was also found that as the heights of two flat fences were increased, a limit is reached above which equilibrium points cannot be found. This does not mean that a solution does not exist for some other combination of fence heights and curvature, but these solutions may be hard to find. The results do indicate clearly that a solution does not exist if the fences are too high. Such an observation seems physically reasonable because, if the fences are too high, no vortex/source combination is capable of controlling the flowfield both over the fences and in the cavity between the fences.

Method Used to Find Zero-Sink Solutions

Results presented previously[24,25] indicate how the front and rear fences affect the source or sink strength required for vortex trapping on both a flat plate and a Clark-Y airfoil. They also indicate how the source strength required for the equilibrium condition can be made negligible by adjusting the heights of the front and/or rear fence. Each fence is noted to contribute differently to the source flow required for equilibrium. It was demonstrated[25] that two fences can be used to control the mass removal so that the drag associated with the vortex trapping process can be made negligible.

The procedure that was used to calculate the flowfield over an airfoil with a trapped vortex consists of several steps.[25] In the first step, the length of the two fences is set to zero so that only the front and rear stagnation points of the vortex bubble are specified. In such a case, the vortex bubble is assumed to have conforming fences that do not interfere with the equilibrium condition (Fig. 5). (A conforming fence is assumed to have zero thickness and to fit, or conform, so closely to the surface of the vortex bubble that the flowfield characteristics are unchanged by addition of the fence.) If the resulting solution shows that a sink is required in order to achieve equilibrium, the height of the rear fence is iteratively increased until the sink flow is negligibly small. Conversely,

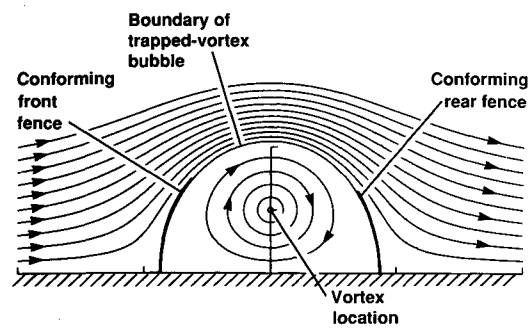

Fig. 5 Vortex trapped on infinite plane to illustrate conforming fences.

if the flowfield solution for the initial conforming-fence geometry requires a source rather than a sink, the height of a flat front fence is increased until $\dot{m} = 0$. This procedure was used to obtain all of the $\dot{m} = 0$ trapped-vortex solutions presented here.

The solutions presented herein were found by the foregoing process because they require the minimum amount of flat-fence material. In theory, only a front or a rear fence is needed to render the required source equal to zero. In practice however, a second fence (front or rear) is needed to control either the front or rear stagnation point of the flowfield of the trapped vortex, even though the second fence is not needed as a reflection plane for the vortex. The flowfields presented in the figures to follow will have only one fence that is approximately flat, and that is needed as a reflection plane to make $\dot{m} = 0$. The tip of the fence that is nearly flat is denoted by a small gap between it and the streamline that departs from the tip. The other fence is not shown, but is assumed to be of the conforming type that is thin and fits the vortex bubble closely. A more complete analysis or experiment will be needed to determine the minimum size for the conforming fence.

Aerodynamic Characteristics of Trapped-Vortex Airfoils

Data Base

In order to obtain a set of solutions that can be used to study the characteristics of airfoils with trapped vortices, a sequence of $\dot{m} = 0$ cases was calculated for the flow over a Clark-Y airfoil at angles of attack from $\alpha = -4$ deg through $\alpha = +12$ deg in increments of 2 deg. Since the streamlines for the various solutions do not change very much, only the solutions for $\alpha = +4$ deg are presented in Fig. 6. The various solutions differ from one another in that the size of the trapped-vortex bubble increases gradually from zero to a size that covers nearly the entire upper surface of the airfoil. The sequence of figures are arranged to represent a portion of the flowfield as the wing is changed from its cruise configuration (i.e., no vortex) to the high-lift configuration with a vortex-bubble needed for landing. For takeoff, the sequence is reversed so that the fences are first deployed so as to develop the size of trapped-vortex needed for high lift. As the aircraft becomes airborne and increases its flight velocity, the fences would change so that the vortex bubble shrinks in size progressively until the cruise configuration is achieved.

Minimum Height of Flat Fences

The first parameter to be discussed is the height of the flat fence used to bring about the $\dot{m} = 0$ condition (Fig. 7). The parameters that are used to define the chordwise extent of the vortex bubble are shown in the inset figure. The chordwise front of the bubble x_f is taken as the intersection of the bubble or fence surface with the upper surface of the airfoil. Similarly, the rear (or downstream) end of the vortex bubble x_r is defined as the aft intersection point on the airfoil. It is noted that a flat fence length of about $0.1c$ is required in order to obtain a vortex bubble that covers 26% of the airfoil. A flat rear fence length of about $0.2c$ produces a vortex bubble that covers about half of the airfoil surface. This figure and the previous one clearly show that the size of the vortex bubble is controlled by the spacing between the front and rear fences.

Effect of Bubble Size on Lift

The lift coefficient developed by the various trapped-vortex configurations is presented in Fig. 8 for the range of vortex bubble sizes that were studied. It is noted that the lift increases slowly at first as the size of the vortex bubble increases from zero. Then, at the larger bubble sizes, the lift changes rapidly. Also, note that not all of the curves end at the largest vortex-bubble sizes. The computations indicate that it is not possible to find an equilibrium point for $\dot{m} = 0$ in certain cases. A physical reason for the solution failure was not found, but it

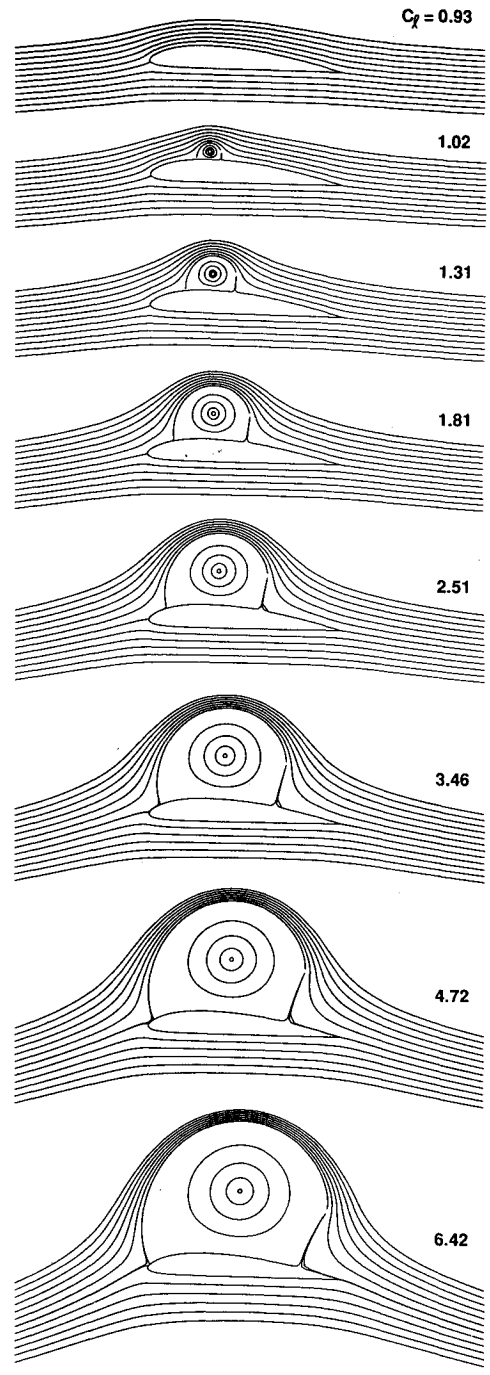

Fig. 6 Streamline plots of flow about Clark-Y airfoil for a range of sizes of a trapped-vortex bubble for high lift; $\dot{m} = 0$, $\alpha = 4$ deg. Front fence is a conforming fence.

seems reasonable that fence heights above certain values should not be possible solutions because the fences begin to interfere with the vortical flowfield and cause it to become too distended in the vertical direction.

It is apparent that the curves in Fig. 8 are similar in shape. In an effort to collapse Fig. 8 to a single curve, the lift increment due to the trapped vortex (rather than the total lift) is plotted as a function of the size of the vortex bubble $(x_r - x_f)/c$ (Fig. 9). Unfortunately, complete correlation occurs only for the smaller values of $(x_r - x_f)/c$. As the vortex bubble size increases, the difference between the curves also increases. Better correlation appears to be achieved when the lift is based on the area enclosed by the vortex bubble or on the square of the streamwise extent of the vortex bubble. Since any one of the parameters chosen for correlation is a bit arbitrary in its definition and the benefit of perfect cor-

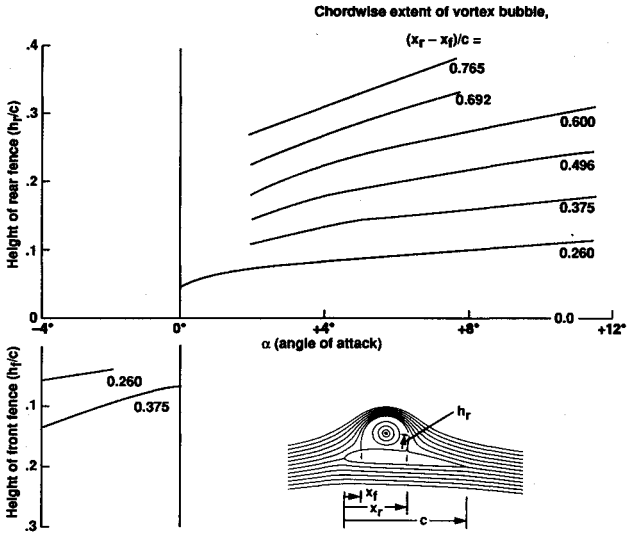

Fig. 7 Length of fence as a function of angle of attack for several trapped-vortex bubble sizes, $(x_r - x_f)/c$.

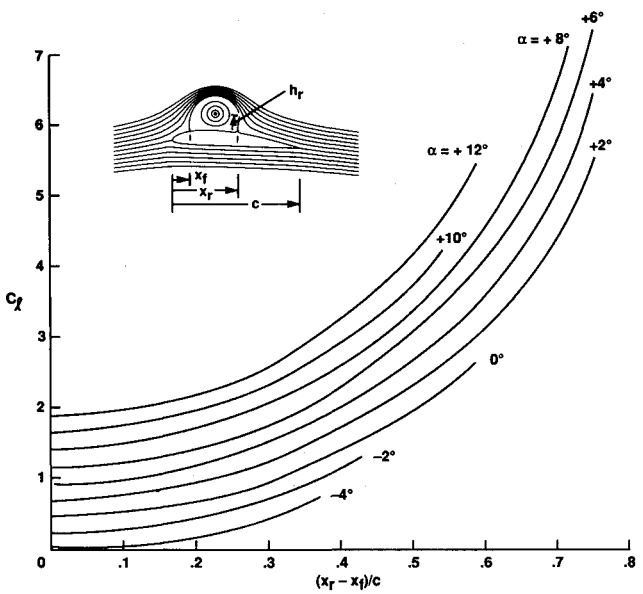

Fig. 8 Lift coefficient as a function of distance between fence attachment points for several angles of attack; h_r or h_f adjusted so that $\dot{m} = 0$.

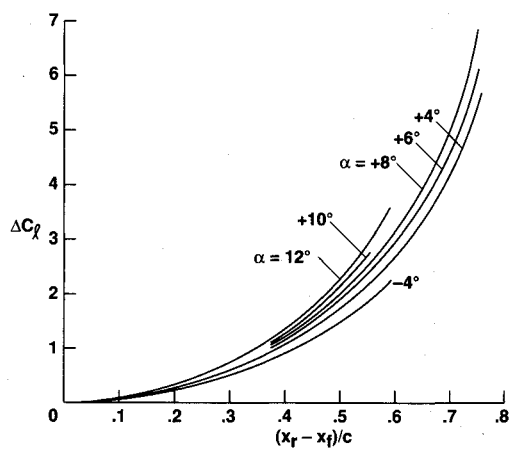

Fig. 9 Increment in lift coefficient due to addition of trapped vortex as a function of distance between fence attachment points for several angles of attack; h_r or h_f adjusted so that $\dot{m} = 0$.

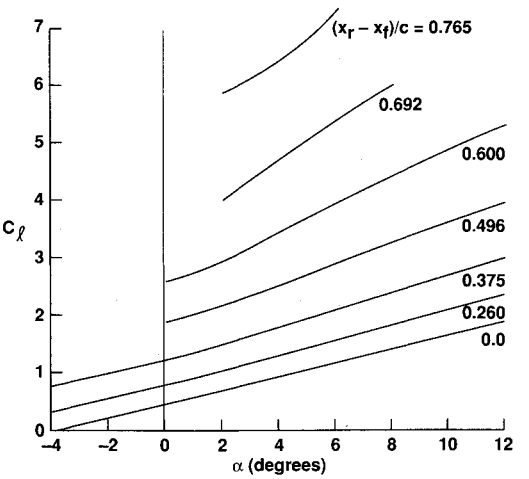

Fig. 10 Lift coefficient as a function of angle of attack for several values of the distance between fence attachment points; h_r or h_f adjusted so that $\dot{m} = 0$.

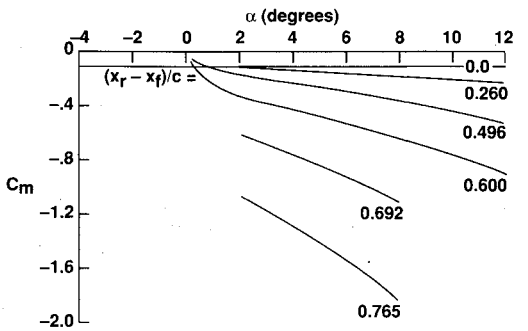

Fig. 11 Pitching-moment coefficient as a function of angle of attack for several values of the distance between fence attachment points; h_r or h_f adjusted so that $\dot{m} = 0$.

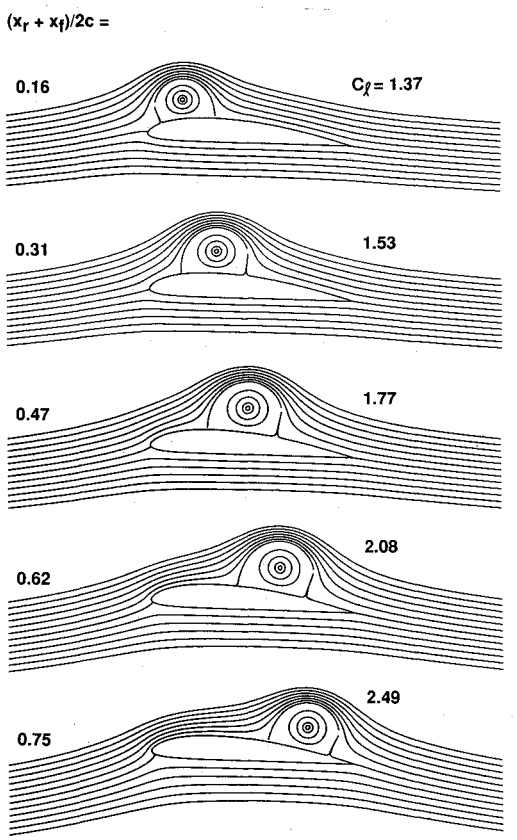

Fig. 12 Streamline plots of flow about Clark-Y airfoil for a range of chordwise locations of trapped-vortex bubble, $(x_r + x_f)/2$; $\alpha = 4$ deg. Second fence is a conforming fence.

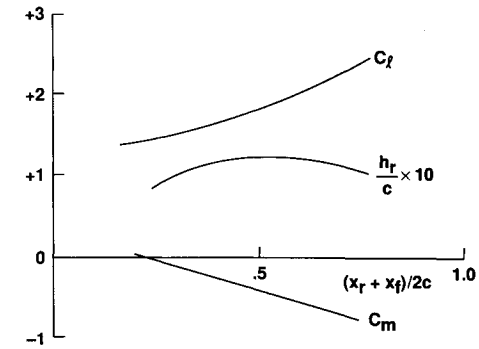

Fig. 13 Characteristics of airfoil as a function of chordwise location for fence attachment points, $(x_r + x_f)/2$; $\alpha = 4$ deg.

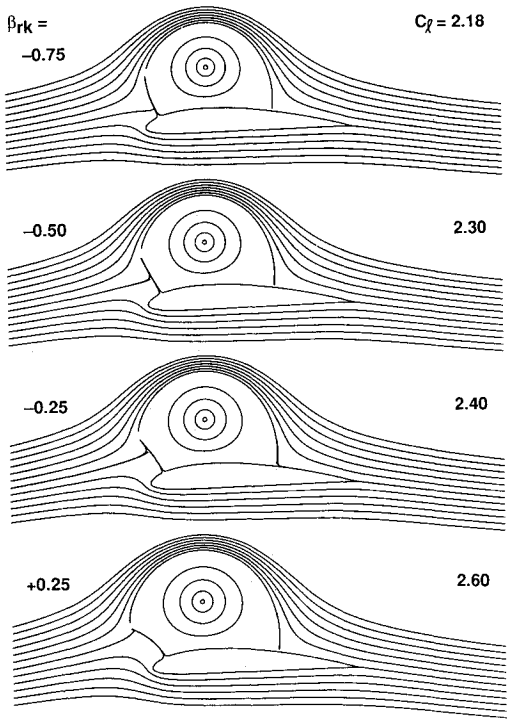

Fig. 14 Streamline plots for flow about Clark-Y airfoil for several values of fence curvature parameter, β_{rk}; $\alpha = 4$ deg. Rear fence is a conforming fence.

relation is not apparent, it seems sufficient to consider the lift enhancement achieved by a trapped vortex to be roughly proportional to the area of the vortex bubble that it produces on the airfoil.

Effect of Angle of Attack on Lift

Figure 10 presents the lift produced as a function of angle of attack for various sizes of the trapped-vortex bubble. It is noted that the variation of lift with angle of attack for bubble sizes that are 60% or less of the chord are approximately linear with angle of attack. The slope of the lift curve increases with increasing size of the vortex bubble. These results indicate that trapped-vortex airfoils have a conventional response to angle of attack. Figure 10 also provides an estimate of the reduction in angle of attack that can be achieved by adding a trapped vortex to the flowfield over the airfoil while retaining the same lift. For example, addition of a trapped vortex that covers 26% of the airfoil, permits about a 4-deg reduction in angle of attack with no change in the lift.

Pitching Moment

The pitching moment about the quarter-chord location is expected to vary greatly when the vortex bubble is large and moves aft. Even though an attempt was made to keep the center of the vortex bubble at about the same chordwise station, the pitching moment is seen to become quite large (Fig. 11). Latitude is available, however, for placing the vortex bubble fore or aft on the airfoil to influence the pitching moment. As illustrated by the sequence of trapped-vortex cases presented in Fig. 12, the vortex bubble can be moved fore and aft on the airfoil by large amounts. In Fig. 12, the size of the trapped-vortex bubble is held approximately constant as the chordwise location of the bubble is moved aft in a series of steps from a very forward location (Fig. 13). Some control of the pitching moment is demonstrated by moving the location of the vortex bubble. The lift generated by the trapped vortex decreases at the more forward location, but not disastrously. The minimum height or length of the flat fence also changes somewhat with the location of the trapped vortex, but not significantly.

Effect of Fence Curvature

Emphasis has been placed in the preceding text on the reflection property of the flat fence and on the conforming fence that is used to enclose the trapped vortex. Unfortunately, the mapping method used in the present analysis does not have the capability to shape a fence as desired. It does have the capability, however, to curve the fence both fore and aft a considerable amount.[24,25] In order to illustrate the changes brought about in the flowfield by changes in fence shape, several cases are presented in Fig. 14 for a range of

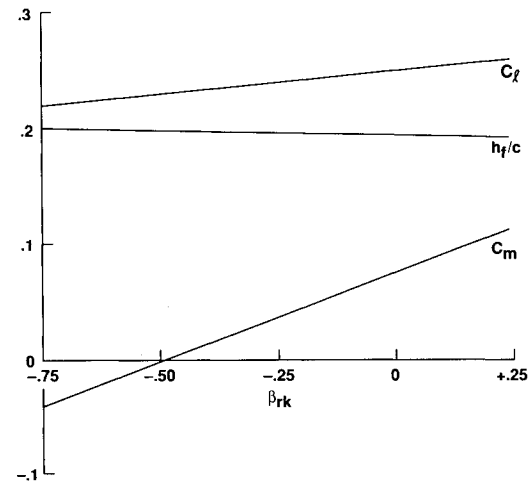

Fig. 15 Characteristics of airfoil as a function of fence curvature parameter, β_{rk}; $\alpha = 4$ deg.

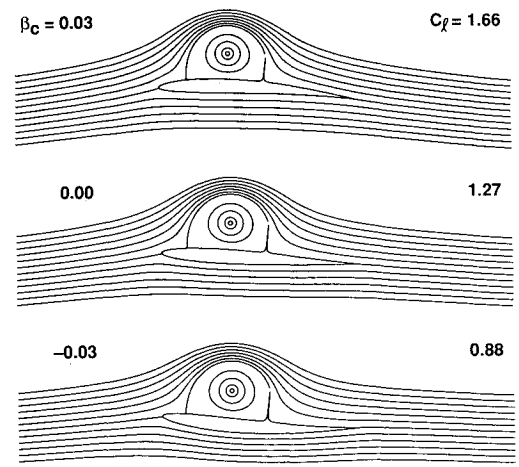

Fig. 16 Trapped-vortex solutions for flowfield of extended Joukowski airfoils with three different values of camber to illustrate application to other airfoils; $\alpha = 4$ deg, $\tau = 0.06$, $\delta = 0.06$. Front fence is a conforming fence.

values of the fence curvature parameter, β_{rk}. The aerodynamic characteristics of these configurations are plotted in Fig. 15. The pitching moment appears to be affected somewhat, but the lift and fence height are insensitive to β_{rk}.

Other Airfoil Shapes

The results presented here and in a previous paper[25] studied the flowfields of both a flat plate airfoil and a Clark-Y airfoil. There appears to be no reason why the trapped vortex could not also be made to occur on a wide variety of other airfoil shapes. In order to illustrate some possibilities, the streamlines for an extended Joukowski airfoil[28] with three different values for the camber are presented in Fig. 16. The size and location of the vortex bubble is the same in all three cases. The total lift differs between the cases, but the lift increment due to the trapped vortex in all three cases is close to $\Delta C_\ell = 0.8$.

Concluding Remarks

An overview has been presented of the characteristics of one airfoil shape which has its lift enhanced by a trapped-vortex flowfield. The research to date suggests that two spanwise fences be used to enclose the trapped vortex, and that the fence heights be adjusted so that the equilibrium condition can be achieved with little or no mass removal from the core region of the vortex. Not only does the configuration not have drag associated with the trapping process, but the vortex is easier to form and appears to be much more stable than if only a front fence is present. The data presented here considered vortex bubble sizes that ranged from zero to a size that covers nearly the entire upper surface of the airfoil. Although perfect correlation was not found for the lift increase due to the trapped vortex, it appears that the lift enhancement is roughly proportional to the cross-sectional area of the trapped-vortex bubble. The results also show that the vortex bubble can be located fore and aft on the airfoil to control aerodynamic parameters such as the pitching moment. Even though situations can be found wherein only a forward or rear fence is needed to produce a zero mass flow condition, both a front and rear fence will probably be used in practice to help stabilize the vortex flowfield. Some effort was devoted to the effect of fence curvature on the aerodynamics of the airfoil, but further study is required in order to better understand the effect of fence shape on the vortex-trapping process. This information provides some necessary steps toward finding the necessary and sufficient conditions for vortex trapping on wings. A possible extension of the single trapped-vortex geometry to two or more trapped vortices on the upper surface of an airfoil may provide the same lift with less cumbersome equipment. Finally, the progression from the two-dimensional configurations studied here to the full three-dimensional flowfield of a wing will no doubt require additional guidelines in order to promote the formation of a vortex that has negligible drag due to vortex trapping, and that is easily formable and stable.

References

[1]Prandtl, L., and Tietjens, O. G., *Applied Hydro- and Aero-Mechanics*, McGraw-Hill, New York, 1934, pp. 155, 156, 279–287.

[2]Wolff, E. B., "Preliminary Investigation of the Effect of a Rotating Cylinder in a Wing," NACA TM 307, 1925; reprinted from De Ingenieure, No. 49, Dec. 6, 1924, pp. 57–66.

[3]Betz, A., "Recent Experiments at Goettingen Aerodynamic Institute," NACA TM 310, 1925; reprinted from Zeitschrift des Vereines deutscher Ingenieure, Jan. 3, 1925, pp. 9–14.

[4]Ackeret, J., "Recent Experiments at Goettingen Aerodynamic Institute," NACA TM 323, 1925; reprinted from Zeitschrift fuer Flugtechnik und Motorluftschiffahrt, Feb. 14, 1925, pp. 44–52.

[5]Wolff, E. B., and Konig, C., "Tests for Determining the Effect of a Rotating Cylinder Fitted into the Leading Edge of an Airplane Wing," NACA TM 382, 1926; reprinted from Report A.105 of the Rijks-Studiedienst Voor de Luchtvaart, Amsterdam, 1926.

[6]Frey, K., "Experiments with Rotating Cylinders in Combination with Airfoils," NACA TM 382, 1926; reprinted from Zeitschrift fuer Flugtechnik und Motorluftschiffahrt, Aug. 28, 1926, pp. 342–345.

[7]Van der Hegge Zijnen, B. G., "Determining the Velocity Distribution in the Boundary Layer of an Airfoil Fitted with a Rotary Cylinder," NACA TM 411, 1927; reprinted from De Ingenieur, Oct. 23, 1926.

[8]Ringleb, F. O., "Separation Control by Trapped Vortices," *Boundary Layer and Flow Control*, edited by G. V. Lachmann, Vol. 1, Pergamon, London, 1961, pp. 265–294.

[9]Hurley, D. G., "The Use of Boundary Layer Control to Establish Free Stream-Line Flows," *Boundary Layer and Flow Control*, edited by G. V. Lachmann, Vol. 1, Pergamon, London, 1961, pp. 265–294.

[10]Krall, K. M., and Haight, C. H., "Wind Tunnel Tests of a Trapped Vortex-High Lift Airfoil," Advanced Technology Center, Rept. B-94300/3TR-10, Dallas, TX, Dec. 1972.

[11]Gleason, M., and Roskam, J., "Preliminary Results of Some Experiments with a Vortex Augmented Wing," SAE Paper 720321, National Business Aircraft Meeting, Wichita, Kansas, March 1972.

[12]Cox, J., "The Revolutionary Kasper Wing," *Sport Aviation*, Vol. 11, July 1973, pp. 10–16.

[13]Kasper, W. A., "Some Ideas of Vortex Lift," National Business Aircraft Meeting, Society of Automotive Engineers Paper 750547, Wichita, KA, April 8–11, 1975.

[14]Chang, P. K., *Control of Flow Separation*, McGraw-Hill, New York, 1976, pp. 291–297, 412–444.

[15]Kruppa, E. W., "A Wind Tunnel Investigation of the Kasper Vortex Concept," AIAA Paper 77-310, Jan. 1977.

[16]Saffman, P. G., and Sheffield, J. S., "Flow over a Wing with an Attached Free Vortex," *Studies in Applied Mathematics*, Vol. 57, No. 2, 1977, pp. 107–117.

[17]Mattick, A. A., and Stollery, J. L., "Increasing the Lift:Drag Ratio of a Flat Delta Wing," *Aeronautical Journal*, Vol. 85, No. 848, 1981, pp. 379–386.

[18]Saffman, P. G., and Tanveer, S., "Prandtl-Batchelor Flow Past a Flat Plate with a Forward-Facing Flap," *Journal of Fluid Mechanics*, Vol. 143, June 1984, pp. 351–365.

[19]Saffman, P. G., and Tanveer, S., "Vortex Induced Lift on Two Dimensional Low Speed Wings," *Studies in Applied Mathematics*, Vol. LXXI, No. 1, 1984, pp. 65–78.

[20]Rao, D. M., and Johnson, T. D., Jr., "Investigation of Delta Wing Leading-Edge Devices," *Journal of Aircraft*, Vol. 18, No. 3, 1981, pp. 161–167.

[21]Lamar, J. E., Schemensky, R. T., and Reddy, C. S., "Development of a Vortex-Lift Design Procedure and Application to a Slender Maneuver-Wing Configuration," *Journal of Aircraft*, Vol. 18, No. 4, 1981, pp. 259–266.

[22]Marchman, J. F., III, "Effectiveness of Leading-Edge Vortex Flaps on 60 and 75 Degree Delta Wings," *Journal of Aircraft*, Vol. 18, No. 4, 1981, pp. 280–286.

[23]Reddy, C. S., "Effect of Leading-Edge Vortex Flaps on Aerodynamic Performance of Delta Wings," *Journal of Aircraft*, Vol. 18, No. 9, 1981, pp. 796–798.

[24]Rossow, V. J., "Lift Enhancement by an Externally Trapped Vortex," *Journal of Aircraft*, Vol. 15, No. 9, 1978, pp. 618–625.

[25]Rossow, V. J., "Two-Fence Concept for Efficient Trapping of Vortices on Airfoils," *Journal of Aircraft*, Vol. 29, No. 5, 1992, pp. 847–855.

[26]Wadcock, A. J., Bennett, M. S., and Smith, C. A., "An Efficient Micro-Computer System for the Analysis of Particle Image Velocimetry Specklegrams," AIAA Paper 91-3246, Sept. 1991.

[27]Riddle, T. W., Wadcock, A. J., Tso, J., and Cummings, R. M., "Experimental Analysis of Vortex Trapping Techniques," AIAA Paper 91-3271, Sept. 1991.

[28]Streeter, V. L., *Fluid Dynamics*, McGraw-Hill, New York, 1948, pp. 150–155.